EPJ E
Soft Matter and Biological Physics
EPJ.org
your physics journal

Eur. Phys. J. E **29**, 239–244 (2009) DOI: 10.1140/epje/i2009-10474-x

Spreading of diblock copolymer droplets: A probe of polymer micro-rheology

A.B. Croll and K. Dalnoki-Veress

EDP SCIENCES
Società Italiana di Fisica
Springer

Eur. Phys. J. E **29**, 239–244 (2009)
DOI 10.1140/epje/i2009-10474-x

THE EUROPEAN PHYSICAL JOURNAL E

Regular Article

Spreading of diblock copolymer droplets: A probe of polymer micro-rheology

A.B. Croll and K. Dalnoki-Veress[a]

Department of Physics & Astronomy and the Brockhouse Institute for Materials Research, McMaster University, Hamilton, ON, Canada

Received 4 March 2009 and Received in final form 4 May 2009
Published online: 24 June 2009 –

Abstract. We present an experimental study of the spreading dynamics of symmetric diblock copolymer droplets above and below the order-disorder transition. Disordered diblock droplets are found to spread as a homopolymer and follow Tanner's law (the radius grows as $R \sim t^m$, where t is time and $m = 1/10$). However, droplets that are in the ordered phase are found to be frustrated by the imposed lamellar microstructure. This frustration is likely at the root of the observed deviation from Tanner's law: droplet spreading has a much slower power law ($m \sim 0.05 \pm 0.01$). We show that the different spreading dynamics can be reconciled with conventional theory if a strain-rate–dependent viscosity is taken into account.

PACS. 83.80.Uv Block copolymers – 68.08.Bc Wetting – 82.35.Gh Polymers on surfaces; adhesion – 47.55.D- Drops and bubbles

1 Introduction

The spreading of liquid droplets on solid substrates has long fascinated many researchers [1–8]. A firm understanding of the details governing droplet dynamics is crucial for many industrial processes and serves as a testing-ground for the physics of capillarity [1]. The wetting of a surface by droplets of simple fluids [2–4], as well as more complex polymeric fluids [5–8] has therefore received much attention.

Tanner, who studied the spreading of poly(dimethylsiloxane) droplets, noted that the apparent contact line of the droplets spread in time with the characteristic power law of t^m; where $m = 1/10$ —commonly referred to as Tanner's law [2]. Tanner also discussed the complexities of a hydrodynamic solution due to divergences in the vicinity of the contact line, which is related to a nanoscopic precursor film that spreads diffusively ahead of the contact line of the droplet (see fig. 1). The existence of the precursor film was suggested by the earlier experiments of Hardy [9], and this film was found to cover the substrate quickly compared to the spreading of the bulk droplet. As a result the macroscopic wetting that is observed is a consequence of the bulk droplet spreading on a microscopic film of the same material, thus removing the chemical details of the surface from the problem.

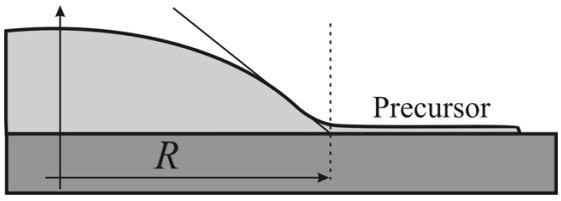

Fig. 1. The geometry of a spreading droplet with radius, R, volume, Ω, surface tension, σ, and viscosity, η. Also illustrated is a precursor wetting layer which spreads ahead of the bulk droplet.

The dynamics of wetting was put on firm theoretical footing by de Gennes who developed a hydrodynamic theory which correctly predicted the scaling relationship

$$R(t) \sim \left(\frac{\sigma}{\eta}\right)^{\frac{1}{10}} \Omega^{\frac{3}{10}} t^{\frac{1}{10}}, \tag{1}$$

where R is the position of the apparent contact line, σ is the surface tension, η is the viscosity, and Ω is the droplet volume [10]. In this formalism, the energy gained by spreading is balanced by the energy lost to viscous dissipation in a wedge of fluid near the apparent contact line of the drop. The universality of the wetting dynamics was shown by de Gennes to be due to the presence of the precursor layer. As a result of this layer, the droplet spreads with a power law that is independent of the substrate. Since the energy gained by covering the substrate surface

[a] e-mail: dalnoki@mcmaster.ca

is dissipated in the precursor film alone, the droplet dynamics is entirely due to the Laplace pressure reducing the curvature of the droplet as it spreads on the precursor.

Diblock copolymers, molecules made of two chemically distinct polymer blocks with monomers "a" and "b" covalently bonded to one another, are widely studied and find increased use as a compatibilizing agent between two surfaces (for example as a coating on an unfavorable substrate) due to their amphiphilic nature [11–13]. Because of the chemical incompatibility of polymer blocks a and b, diblock copolymers are found to phase separate as they pass through the order-disorder transition (ODT). The connectivity of the blocks limits the length scale of the phase-separated domains to that of the molecular size ($\sim 10\,\mathrm{nm}$). The geometry of the morphology depends on the natural curvature induced by the ratio of the two block lengths and the stretching of the chains required to accommodate the morphologies with long-range periodic order. Here we deal with the simplest case: a symmetric diblock where the a and b components are of equal size favouring the zero-curvature microstructure of lamellae [12,14]. The phase transition as the system passes through ODT is most easily understood through changes in the temperature, T: high temperature favours the entropy of the polymer coils as they randomly fill space, whereas at low temperature the enthalpy dominates which drives the segregation of the blocks to minimize a and b contacts. Though somewhat less intuitive, ODT can also be traversed through changes in molecular weight. In this case increasing the molecular weight, M_N, leads to increasing the enthalpic contribution and hence ordering; this is because the energy cost of removing a block from its preferred domain is proportional to its size. Thus, the ordered state can be obtained by increasing the molecular weight of the molecules or by decreasing T. These two effects are generally combined as χN, where N is the number of segments in a chain, and χ is the Flory-Huggins interaction parameter (typically written as $\chi = A/T + B$).

The microstructure of a block copolymer melt significantly changes its rheology [11,16]. When in a disordered state a diblock copolymer responds much like a homopolymer and the timescales of flow are set by the length of the polymer. When microphase separation takes place, the structure imposed on the fluid adds complexity to its rheological response (for example, see fig. 6 of [11]). One might expect the addition of structure to result in an additional barrier to flow, which naturally raises several questions: Does the underlying structure affect droplet spreading in an observable way? Can the flow of diblock copolymer droplets be understood in the same manner as that of more simple fluids? Here we address these questions with an experimental study of the spreading of symmetric diblock copolymer droplets. We find that the droplet spreading is comparable to simple polymeric fluids when the polymer is in the disordered state, while the flow during spreading is significantly impeded in the ordered state. The slow dynamics observed here can be understood when the spreading dynamics theory of de Gennes is coupled with a viscosity that is dependent on the microstructure.

Table 1. Polymer details: the number-averaged molecular weights for the PS and PMMA blocks, the polydispersity index, and the microstructural state at 180 °C (D: disordered, O: ordered) [17].

M_N^{PS} (kg/mol)	M_N^{PMMA} (kg/mol)	PI	Phase
10.0	10.0	1.05	D
12.8	12.9	1.05	D
14.9	13.1	1.05	O
18.0	18.0	1.07	O
25.0	26.0	1.09	O
52.0	52.0	1.09	O

2 Experiment

Electronics grade Si substrates (University Wafer, USA) with the native oxide layer present were cleaned with super critical CO_2 ("Snow jet", Applied Surface Technologies, USA) and UV-ozone treatment, which will largely eliminate surface contamination. The resulting substrates were completely wetted by the polymers used in this study: a series of symmetric monodisperse poly(styrene-methyl methacrylate) (PS-PMMA) of various total M_N, obtained from Polymer Source (Dorval, Quebec). Details of the polymers used in this study can be seen in table 1. We note that when we discuss the molecular weight of a system we refer to the total weight of the molecule, with each block composing half of the total mass. There is a slightly lower interfacial tension between PMMA and the substrate than that of PS and the substrate. Furthermore, PS has a lower surface tension than does PMMA at the temperatures studied. As a result, when ordered, the wetting precursor layer on the substrate is a monolayer allowing PMMA contact with the substrate and PS with air. All additional layers will be bilayers in order to maintain a PS-air interface *i.e.* Si/PMMA-PS/PS-PMMA PMMA-PS/etc.

The PS-PMMA was "dusted" onto a substrate, heated, and observed via optical microscopy. Several molecular weights were used, ranging from molecules with 20 kg/mol to 104 kg/mol. From previous work it was known if the droplets were in the ordered or disordered state (see table 1 for the details) [17]. All experiments were carried out on a microscope hot stage (Linkam Scientific, UK) at 180 °C as well as in a separate home-built vacuum oven. Some substrates were spin-coated with a monolayer of diblock from a dilute polymer solution in toluene prior to use. Since a monolayer precursor film is expected to form ahead of the spreading droplet, comparison of droplet spreading on either substrate should be equivalent. There was no difference between the spreading dynamics of experiments on the Si substrate or those pre-coated with a monolayer. The test on the two substrates shows unambiguously that there is a precursor layer in front of the bulk droplet and that the final state is a totally wet substrate.

Droplet radii were measured with reflection optical microscopy. White light was filtered with a green notch filter

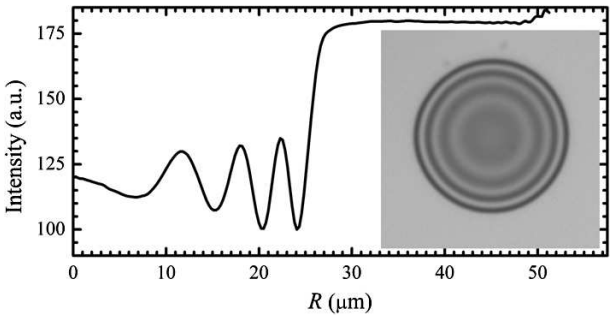

Fig. 2. An average intensity profile from a typical droplet (shown in inset). In this case the droplet is made up of a 20 kg/mol disordered diblock copolymer.

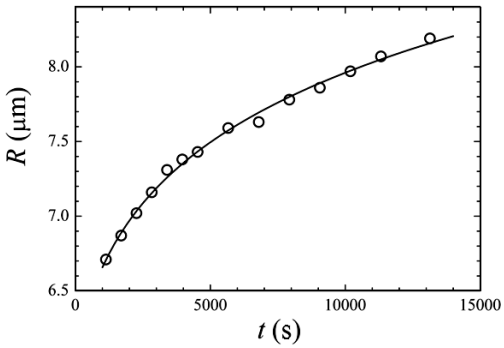

Fig. 3. Radius as a function of time for the spreading of a typical disordered diblock copolymer droplet. Shown is data from a 20 kg/mol droplet on a Si substrate. The curve is a power law fit with exponent 0.096 ± 0.004.

(centered at 533 nm, FWHM 10 nm) in order to improve our measurements which depend on interference fringes. Software was developed which located a droplet center and then averaged the interference fringes of the droplet around this point (see fig. 2). The fringes were converted into topography data and fit with the generic equation $0 = Ax^2+Bxy+Cy^2+Dx+Ey+F$. Fitting to this droplet profile was used because we have previously found that ordered droplets can have a hyperbolic profile; thus this simple form is valid in the case of hyperbolic or spherical cap droplets and can be used to determine the state of order [17]. The fit function was extrapolated to the substrate to yield the dynamic contact angle, θ_D, and radius of the contact line, R. Since the bulk droplet "leaks" into the precursor layer, by accessing both θ_D and R, the droplet volume could be monitored thereby ensuring that the volume of the droplet was constant as required in the theory. The use of the interference fringes limits the droplets included in this study to those such that the fringes nearest the edge could still be easily resolved (contact angles $< 30°$).

Atomic force microscopy (AFM) was used in order to independently verify the microstructure of the droplets and contact angle (Caliber, Veeco, USA). These measurements involved quenching samples to room temperature, well below the glass transition, and then scanning with tapping mode with AFM. No significant deviations from the optical experiments were found.

3 Results and discussion

3.1 Disordered droplets

A typical spreading curve for a disordered diblock copolymer can be seen in fig. 3. The solid line is a fit to the power law $R(t) \sim (t-t_0)^m$, where m and t_0 are fitting constants. The time offset is crucial because the start of flow is not clearly defined both because the drop does not start as a perfect spherical cap and because the time at which the flow begins is not exactly when the accumulation of images starts. The radius is found to grow as a power law in time with an exponent of 0.096 ± 0.004 —a scaling that is consistent with the spreading of simple fluids and homopolymers in accordance with Tanner's law. This scaling was typical of all droplets studied in the disordered regime ($M_N = 20$ and 26 kg/mol).

The rheology of homopolymers is well known to be non-linear, particularly if the polymer length is above the entanglement length, where the polymer diffusion becomes significantly slowed by the topological constraints imposed by other chains [19]. In general the polymer viscosity will depend on the shear strain rate and shear thinning is observed beyond some critical shear strain rate. Here we simply estimate the shear strain rate as the spreading velocity divided by the droplet height, H. For the droplet in fig. 3, using the largest velocity, $V/H \sim (0.3\,\text{nm/s})/(800\,\text{nm})$, we estimate the shear rate to be below $\sim 10^{-4}\,\text{s}^{-1}$ over the course of the experiment. Comparison to work by other researchers reveals that this is well below the critical shear strain rate, validating the constant value of the viscosity used in the derivation of Tanner's law and the results obtained in the experiments described here (see fig. 1 of ref. [16] which shows that this system is well within the terminal flow region). With a constant viscosity there is no significant difference in the spreading dynamics between disordered block copolymers and simple fluids, and therefore we can easily understand the good agreement with the predicted 1/10 power law.

3.2 Ordered droplets

Figure 4 shows the radius as a function of time for several droplets of 36 kg/mol molecules. This system is ordered at 180 °C [17]. These droplets flow in a different manner. Initially, spreading is in agreement with Tanner's law —a power law exponent of $\sim 1/10$. However after some time (~ 5000 s) flow crosses over to follow a power law with a lower exponent. This slower spreading has been observed for all the molecular weights studied in the ordered regime (see table 1), on both the Si- and monolayer-covered substrates, in air and under vacuum. The slower spreading region is well fit by an exponent of 0.05 ± 0.01: we stress that the power law scaling is still consistent with the data, but with a smaller exponent than the expected 1/10 value of Tanner's law.

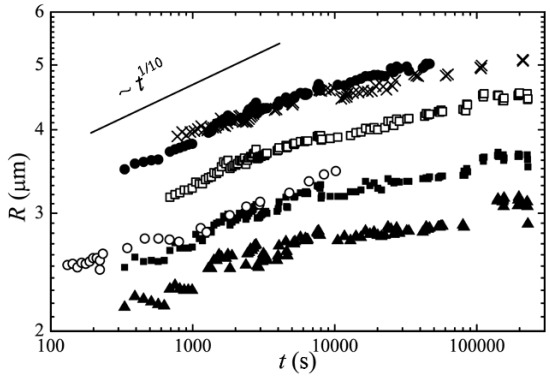

Fig. 4. A double logarithmic plot of the contact radius of several 36 kg/mol diblock copolymer drops of differing volume as a function of time at 180 °C. At this temperature, this system is in the ordered lamellar regime. The observed noise on the signal is related to focal drift over the course of the experiment.

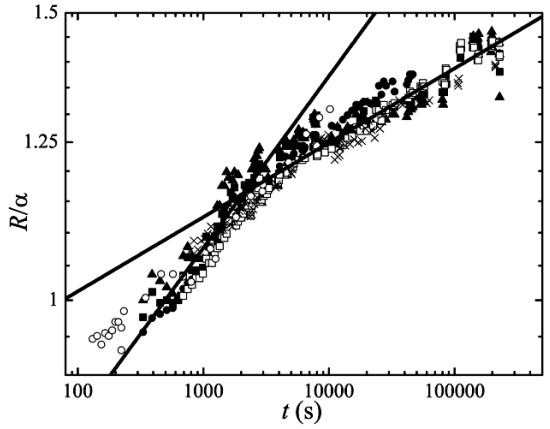

Fig. 5. Data from fig. 4 scaled by dividing by a scaling parameter, α, described in the text. Note that this one parameter is enough for the data to collapse on the same curve. The slopes of the best-fit lines correspond to 0.1 ± 0.01 in the initial fast regime and 0.05 ± 0.01 in the slow regime for 36 kg/mol droplets.

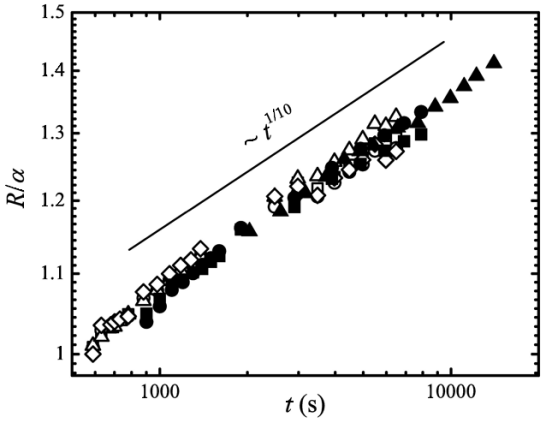

Fig. 6. Data as shown in fig. 5 for the case of diblock droplets with molecular weights which are disordered at the temperature at which the experiments are performed (20 and 26 kg/mol). The data is consistent with the scaling of Tanner's law.

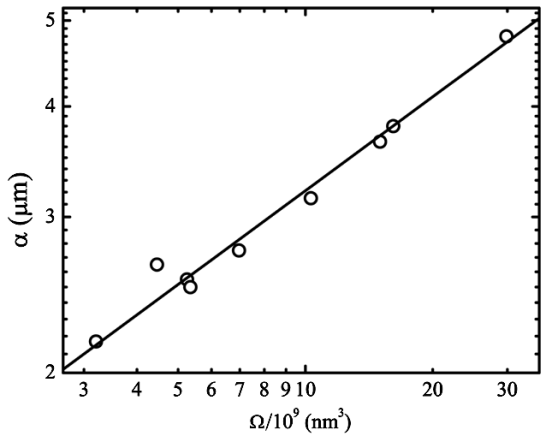

Fig. 7. In this figure we show a log-log plot of the scaling parameter as a function of volume for the 36 kg/mol droplets. The line is a power law fit with a slope of 0.29 ± 0.03.

In fig. 5 we rescale the data of of fig. 4 by normalizing the data by a prefactor, α. The normalization is chosen such that the data sets collapse and correspond to unity at 500 s. The crossover from the "fast" to "slow" regime is clear for the molecular weights that can order. This crossover behaviour should be contrasted with that of the very low molecular weights which remain disordered shown in fig. 6 which show growth consistent with Tanner's law. Comparison with Tanner's law (eq. (1)) reveals that the prefactor is dependent on viscosity, surface tension, and the volume of the drop, $\alpha \sim (\sigma/\eta)^{1/10}\Omega^{3/10}$. Since η and σ are the same for the set of 36 kg/mol droplets shown in fig. 5, we plot the scaling parameter as a function of the volume of the droplets in fig. 7. This is well fit by a power law with an exponent of 0.29 ± 0.03, consistent with that predicted by Tanner's law.

We suggest that the basis of the crossover from Tanner's law to a different power law is the result of increasing ordering in the droplets. In the initial stages of growth the droplets are not well ordered, both because ordering takes time and because the growth rate is most rapid initially which may impede ordering. The initial spreading dynamics is analogous to disordered droplets and hence follows Tanner's law. However, as the spreading proceeds, the velocity decreases and eventually larger length scale lamellae parallel to the substrate start to dominate [17]. Once significant order appears flow is frustrated further, *i.e.* more complex rearrangement of lamellae and polymer molecules in one layer have to overcome a hopping barrier to flow into an other layer [21]. The ordering results in a change in the rheology of the fluid in the droplet —as the droplet velocity slows, order increases, and the effective viscosity increases. This is similar to the increasing viscosity with decreasing frequency of rheological experiments which has been observed in block copolymer samples, see for example [16]. We can estimate the shear strain rate from the data in fig. 4 and the droplet size to be $\sim 10^{-3}\,\mathrm{s}^{-1}$ at the crossover from fast to slow behavior. This is approximately

where the modulus of a block copolymer is known to show power law behavior [16], which suggests that one might expect a non-linear viscosity in the spreading droplet.

Based on the observation that the flow is impeded, we make the following simple assumption: the viscosity varies inversely with the shear strain rate as $\eta \sim \eta'\dot{\gamma}^{-\beta} \sim \eta'(h/V)^{\beta}$, where β is a positive constant, h is the height of the droplet wedge at some point near the contact line, and V is the average velocity of the contact line. We note that this is similar to what is expected for shear thinning fluids and follow the theory presented by Rafaï and coworkers on that topic [22], which we describe briefly here. We take as starting point that the energy that drives the spreading is balanced by the energy dissipated in the fluid wedge at the contact line (see [1,10]),

$$\frac{\sigma\theta_D^2 V}{2} = \int_a^R \int_0^h \eta \left(\frac{\mathrm{d}V}{\mathrm{d}z}\right)^2 \mathrm{d}z\,\mathrm{d}x, \qquad (2)$$

where the driving force comes from the surface tension, σ, and the contact angle, θ_D. The integrals are over the height of the droplet and the radial distance; the details of the small length scale cutoff, a, depends on the molecular scale and is well discussed in [1,10]. Assuming Poiseuille flow, that θ_D is small, and near the wedge $h \sim \theta x$, one obtains

$$R \sim \left(\frac{\sigma}{\eta'}\right)^{\frac{1}{10-3\beta}} \Omega^{\frac{3-\beta}{10-3\beta}} t^{\frac{1-\beta}{10-3\beta}}, \qquad (3)$$

which is in full agreement with the expression obtained by Rafaï and coworkers for shear thinning. Equation (3) represents a modified Tanner's law which includes the possibility of a non-linear viscoelasticity that can be described by $\eta \sim \eta'\dot{\gamma}^{-\beta}$. The best fit to the slow growth regime shows $R \sim t^m$, with $m = 0.05 \pm 0.01$. Since $\beta = (1 - 10m)/(1-3m)$, the non-linear viscosity seen in the spreading experiments corresponds to $\eta \sim \eta'\dot{\gamma}^{-(0.59\pm0.14)}$ [15]. We can compare this result with those obtained previously on bulk samples and find that the droplet spreading non-linear viscosity is consistent with rheological experiments on diblock copolymers which result in $\beta \sim 0.5$ [16]. We note that this exponent is different from what would be expected for the shear thinning of a simple homopolymer, $\eta \sim \eta'\dot{\gamma}^{-1}$ [19].

Finally the lamellar structure's effect on the spreading can be examined with atomic force microscopy (fig. 8). In previous work we have shown that ordered droplets can have a hyperbolic profile when the flow is very slow or halted [17]. Here the morphologies observed are different as flow is still significant and droplets are far from equilibrium. Disordered droplets show the expected spherical shape (see fig. 8b), with a minor perturbation due to weak ordering induced by the substrate [23]. The small amount of order near the substrate is insignificant when compared with the bulk of the droplet and does not seem to affect the flow. The droplets in the ordered state show a complex morphology (see figs. 8a and c), with lamellar grains forming parallel and perpendicular to the substrate. The lack of a single grain of order as observed in our previous work [17] is a dynamical effect —the droplet starts flowing from a relatively disordered state but quickly orders into many lamellar grains. The order, however, only finds the preferred minimum energy state (parallel to substrate) after significant annealing. We have verified the scaling in time of the droplet radius directly with atomic force microscopy, and note no deviation from the results obtained with optical technique.

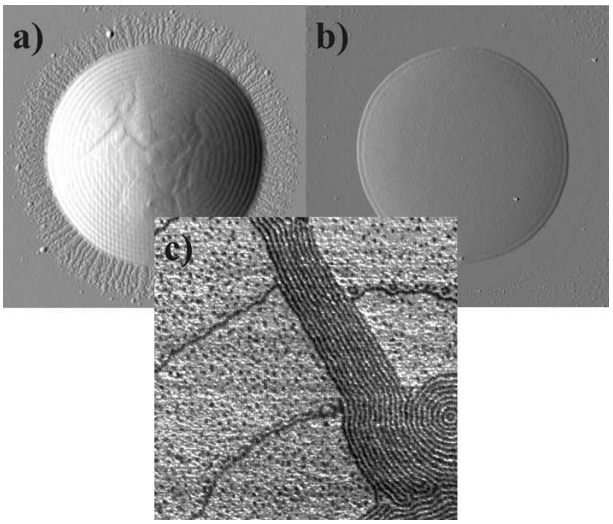

Fig. 8. Atomic force micrographs of several different droplets, illustrating some details of the microstructure. a) A sample image of an ordered droplet (36 kg/mol) in the process of spreading over the substrate (error signal image, 11 μm × 11 μm). The defects near the top of the droplet are due to grains of lamellae organized orthogonal to the substrate. b) A disordered drop (20 kg/mol), which illustrates the spherical nature of the droplet and the small amount of surface-induced ordering (error signal image, 33 μm × 33 μm). c) Close up of a defect near the top of a droplet (phase image, 2 μm × 2 μm).

3.3 Molecular weight effects

We now turn to the effect of molecular weight on the droplet spreading. In order to determine if any molecular weight effects existed in this system, the same master plots as described above were constructed for all ordered samples (see table 1). The scaling parameters were then plotted as a function of volume as can be seen in fig. 9. For all molecular weights except perhaps the 104 kg/mol sample, the data falls along the same power law. Since a vertical shift in these data is related to surface tension and viscosity as seen in eq. (3), the fact that all the data lies on the same general curve may initially seem counterintuitive as homopolymer viscosity is highly molecular-weight–dependent. However, in a partially ordered sample the molecular domains are segregated and spreading takes place mainly through lamella sliding past one another, and the rheology is primarily a result of this microstructure [18]. The viscous losses are therefore determined by the molecular friction of the lamella sliding, an effect that is amplified by shearing [20]. With a small

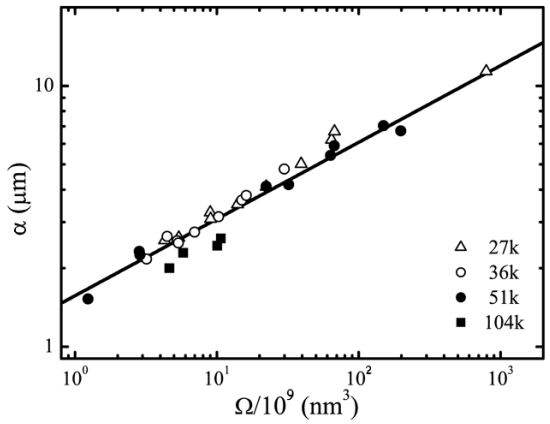

Fig. 9. A log-log plot of the scaling factor α (see text) obtained in the creation of master plots for various molecular weights, as a function of volume. The solid line is a best fit to the data excluding the 104 kg/mol sample $\alpha \sim \Omega^{0.29\pm0.03}$.

interpenetration or entanglement between lamellae, there is no longer any physical reason for molecular weight to contribute as significantly to the flow as for an entangled polymer melt. The highest molecular weight polymer used in this study, 104 kg/mol, does show some small deviations from the general trend, indicating that the greater penetration of chains into adjacent lamellae expected for higher molecular weights may be starting to become important.

4 Conclusions

We have observed a significantly impeaded flow in ordered diblock copolymer droplets. Droplets that consist of a diblock molecular weight that is disordered show spreading dynamics consistent with Tanner's law. However upon increasing the molecular weight and passing into the ordered regime, the droplets initially follow Tanner's law and then proceed with a slower dynamics. We show that the late stage spreading is consistent with a modified spreading law that takes into account the non-linear viscoelastic effects of the ordered diblock copolymer melt. The picture that emerges is one where as the degree of order increases, both because more time has elapsed and because the flow proceeds more slowly, the droplets crossover from a faster to a slower growth dynamics. The slowing is then related to the frustration induced by the lamellar microstructure of the droplets. We show that this effect persists through many ordered molecular weights. Our experiments show no dependence of the spreading on the molecular weight of the diblock when ordered with a possible exception of the highest molecular weight studied. This suggests, in agreement with other studies, that the character of this fluid is primarily a result of the lamellar structure, and the sliding of lamellae, not of the polymeric nature of the material.

Financial support from NSERC and the ACS PRF are gratefully acknowledged.

References

1. P.G. de Gennes, F. Brochard-Wyart, D. Quéré, *Capillarity and Wetting Phenomena* (Springer-Verlag New York Inc., 2002) pp. 139-151.
2. L.H. Tanner, J. Phys. D: Appl. Phys. **12**, 1473 (1979).
3. M.D. Lelah, A. Marmur, J. Colloid Interface Sci. **82**, 518 (1981).
4. G. He, N.G. Hadjiconstantinou, J. Fluid. Mech. **497**, 123 (2003).
5. D. Ausserré, A.M. Picard, L. Léger, Phys. Rev. Lett. **57**, 2671 (1986).
6. L. Léger, M. Erman, A.M. Guinet-Picard, D. Ausserré, C. Strazielle, Phys. Rev. Lett. **60**, 2671 (1988).
7. E. Pérez, E. Schäffer, U. Steiner, J. Colloid Interface Sci. **234**, 178 (2001).
8. D.R. Heine, G.S. Grest, E.B. Webb III, Phys. Rev. E **68**, 061603 (2003).
9. W. Hardy, Philos. Mag. **38**, 49 (1919).
10. P.G. de Gennes, Rev. Mod. Phys. **57**, 827 (1985).
11. G.H. Fredrickson, F.S. Bates, Annu. Rev. Mater. Sci. **26**, 501 (1996).
12. M.J. Fasolka, A.M. Mayes, Annu. Rev. Mater. Sci. **31**, 323 (2001).
13. F.S. Bates, G.H. Fredrickson, Annu. Rev. Phys. Chem. **41**, 525 (1996).
14. M.W. Matsen, J. Phys.: Condens. Matter **14**, R21 (2002).
15. With $\beta \sim 0.6$, the scaling of $\alpha \sim \Omega^{0.296}$. This is not discernible from the scaling observed in Tanner's law regime of $\alpha \sim \Omega^{3/10}$ and the reason is that the collapse of the data in fig. 5 works well in both regimes.
16. H. Braun, W. Gleinser, H.-J. Cantow, J. Appl. Polym. Sci. **49**, 487 (1993).
17. A.B. Croll, M.V. Massa, M.W. Matsen, K. Dalnoki-Veress, Phys. Rev. Lett. **97**, 204502 (2006).
18. R.G. Larson, K.I. Winey, S.S. Patel, H. Watanabe, R. Bruinsma, Rheol. Acta. **32**, 245 (1993).
19. W.W. Graessley, Adv. Polym. Sci. **16**, 1 (1974).
20. T.A. Witten, L. Leibler, P.A. Pincus, Macromolecules **23**, 824 (1990).
21. A.B. Croll, M.W. Matsen, A.-C. Shi, K. Dalnoki-Veress, Eur. Phys. J. E **27**, 407 (2008).
22. S. Rafaï, D. Bonn, A. Boudaoud, J. Fluid. Mech. **513**, 77 (2004).
23. A. Menelle, T.P. Russell, S.H. Anastasiadas, S.K. Satija, C.F. Majkrzak, Phys. Rev. Lett. **68**, 67 (1992).